

# Nano-crystallization in Decorative Layers of Greek and Roman Ceramics

Philippe Sciau

**Abstract** Besides metallic nanocrystals of lusterware (Chapter “[Lustre and Nanostructures—Ancient Technologies Revisited](#)”), other nanoscale crystals can be found in ancient ceramics and more specifically in their decorative layers or coatings. These crystals can play a major role in the physical properties of these thin layers or can be an indicator of the manufacturing process. These thin layers are formed during firing and result from physicochemical reactions among the diverse compounds of raw preparation. In general, the firing conditions are not suitable for obtaining large crystals and many of the formed phases have crystal sizes of a few tens nanometres. Over a long period of time and throughout the world, the variety of raw preparations and firing conditions used are so diverse that it is not conceivable to give here an exhaustive rundown. In this chapter, we will focus our attention on some decorative layers of Greek and Roman potteries for which oxide nanocrystals play a key role regarding the optical and/or mechanical properties. These decorations were obtained from clay preparations and their physical properties result directly from the nanocrystalline size and the behaviour of clay minerals.

## 1 Introduction

Metallic lustre decorations of glazed ceramics, which appeared in Mesopotamia during the 9th century AD, are certainly the most famous historical example of controlled nanotechnology for optical devices (cf. Part 1, Chapter “[Lustre and Nanostructures—Ancient Technologies Revisited](#)”). But in fact the use of optical properties of metallic particles is older (Colomban 2009; Sciau 2012). Indeed, transmission electron microscopy (TEM) revealed that the dichroic colouring of the amazing 4th century Roman Lycurgus cup, showed at the British Museum, comes from nanocrystals of an Au/Ag alloy dispersed in the glassy matrix (Barber and Freestone 1990;

---

P. Sciau (✉)  
CEMES, CNRS, Université de Toulouse, Toulouse, France  
e-mail: philippe.sciau@cemes.fr

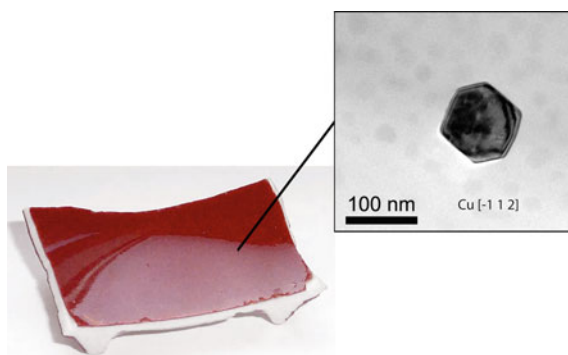
© Atlantis Press and the author(s) 2016  
P. Dillmann et al. (eds.), *Nanoscience and Cultural Heritage*,  
DOI 10.2991/978-94-6239-198-7\_2

Freestone et al. 2007). However, only a few fragments of dichroic glasses were found up to now and none of them has the quality of the glass of the Lycurgus cup. It seems unlikely that sufficient craft experience could have been developed to master this highly complex technology.

In fact, the tinting strength of metallic nanocrystal was used earlier for colouring glasses. It was shown that red glasses of the Final Bronze Age (1200–1000 BC) from Frattesina di Rovigo in Italy were coloured thanks to crystalline particles of metallic copper dispersed in the surface layer of a glassy matrix (Angelini et al. 2004). Many other examples can be found in the literature showing that this glass staining process was widely used worldwide and up to present times. Thus, the presence of both copper and cuprite particles was reported in Celtic enamels (Brun et al. 1991). Most of the Roman tesserae of red colour were obtained from a glass containing copper nanocrystal (Ricciardi et al. 2009). These tesserae were produced massively during the Roman period thanks to a scale production of glass ingots (Colomban 2009). Unlike the manufacturing of the dichroic glasses, the achievement of tinted glass by copper nanoparticles was perfectly mastered by the Roman craftsmen. Outside Europe and the Mediterranean basin, copper nanoparticles for colouring glasses and glazes were also massively used in Asia. For instance, the colouring of Japanese Satsuma glasses was obtained in this way (Nakai et al. 1999). The blue-red Jun glazed porcelains made from Song to Qing Chinese Dynasties were manufactured using a similar process leading to a formation of copper nanocrystals in the red zones during the firing (Wood 1999). It is also the case of some Vietnamese porcelains and celadons (Colomban et al. 2003). The process is still used nowadays. It is at the origin of the glaze colour called oxblood of current porcelains (Fig. 1).

Besides metallic nanocrystals exploited for their optical properties, many other nanoscale crystals such as iron oxides can be found in ancient potteries and more specifically in their decorative or coating layers. These crystals can play a major role in the physical properties of these thin layers or merely be an indicator of manufacturing processes. These thin layers are formed during firing and result from physicochemical reactions among the diverse compounds of raw preparation. In general, the firing conditions are not suitable for obtaining large crystals and many

**Fig. 1** Copper nanocrystal observed in modern porcelain with *red glaze* called “oxblood”



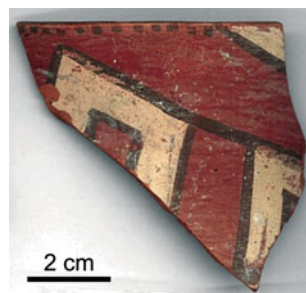
of them have nano or submicrometric sizes. In time and around the world, the variety of raw preparations and firing conditions used are so diverse that it is not reasonable to give here an exhaustive overview. In this chapter, we will focus our attention on some decorative layers of Greek and Roman potteries for which oxide nanocrystals play a key role for the optical and/or mechanical properties. These decorations were obtained from clay preparations and their physical properties result directly from the nanocrystalline size and the behaviour of clay minerals, which are discussed in detail in the next paragraphs, after a short description of the main characteristics of the surface treatments performed from clay preparations.

## 2 Potteries and Surface Treatments

The first potteries, or vessels in fired clay, were made several millennia before the Neolithic revolution in various areas of the world but it is during the Neolithic, with the settlement of human communities, that its use becomes widespread, leading to the improvement of manufacturing processes (Garcia et al. 2014; Sciau and Goudeau 2015). In particular, various surface treatments began to be developed for improving the ceramic properties such as waterproofness or surface strength (hardening). Very early on, these surface treatments had also a decorative function with the design of ornamental patterns, which were specific to cultural communities or civilizations. Since the Neolithic time, knowledge and know-how have improved, leading to the manufacturing of high-quality pottery using very sophisticated surface treatments. Lusterware mentioned in the introduction and presented in detail in Sect. 1.1, is a typical example of achievement with a complex surface treatment requiring two well-controlled firings. The first one allows for the formation of glaze, which provides hardness and tightness while the second leads to the growth of metal nanoparticles within the outermost layers of the glaze (Sciau 2012).

Clay preparations were also intensively used to shape thin decorative and water-resistant coatings at the pottery's surface (Tite 2008). By means of settling and decantation, raw clay material was fractionated to keep only the finest particles and thus to obtain a liquid slip. Then, unfired vessels were dipped into the liquid slip or, the liquid slip was used as paint and applied on the vessel surface. These liquid preparations can be naturally rich in iron if raw clay materials containing oxides and/or hydroxides of iron are selected. Most of these Fe-phases are present in small grains and are kept during the preparation step. Furthermore, several clay minerals (illite, smectite, vermiculite,...) can contain a significant rate of iron in their structures (Deer et al. 1992) and as the clay minerals are also constituted of very small particles, the groundwork results in an increase of the iron rate. The colour after the firing of these slips can be controlled through the redox chemistry of iron so that a firing under reducing conditions leads to a black colour by fostering the formation of magnetite and/or hercynite while a firing under an oxidizing atmosphere leads to a red colour by triggering the formation of hematite. Playing on the total iron rate (preparation), the  $\text{Fe}^{2+}/\text{Fe}^{3+}$  ratio and the size of iron oxide particles formed during

**Fig. 2** Fragment of a Cucuteni ceramic.  
(Micrograph, courtesy D. Popovici and R. Bugoi)



the firing (atmosphere/temperature/time), one can more or less control the final colour from black to bright red. The colour palette can be completed with white slips prepared from raw clay materials containing no iron. The full range was used since the Neolithic times. For example, the flourishing Cucuteni-Tripolye civilization, which was located in the southeastern part of Europe from the Vth to IVth Millennia BC, designed decorative patterns (Fig. 2) using up to 3 colours (Fig. 1) in the same vessel (Bugoi et al. 2008). The red decors were obtained using Fe-rich clay preparations fired under oxidizing conditions at rather a high temperature. To get black colours under these firing conditions, Mn-rich iron minerals were added to the clay preparation, which resulted in the growth of jacobsonite ( $\text{Mn}^{2+}\text{Fe}^{3+}_2\text{O}_4$ ) a black-colour pigment in addition to hematite (Fig. 3).

Some of these slips, especially the ones containing K-rich illitic clay and a high rate of iron (10–20 % in oxide weight), can be easily vitrified during firing and give high-gloss coatings. Those types of surface finishes were especially developed during the Greek and Roman periods (Noble 1965; Tite et al. 1982). It is the basis of the manufacturing of famous Attic ceramics made in Athens and its region from 7th century BC until the late 3rd century BC. Roman craftsmen improved the making of high-gloss red coatings thanks to the focus on kilns permitting a better control of oxidizing conditions leading to the mass production of Terra Sigillata (Hartley 1971; Picon and Vernhet 2008; Sciau et al. 2006). These achievements and the nanostructure of these coatings are detailed in the next sections.

### 3 High Gloss Coatings of Greek and Roman Potteries

#### 3.1 Outlines and Historical Framework

The first high-gloss coatings developed by Greek craftsmen were black and were used to produce beginning the 7th century BC the black-figure pottery painting, also called black-figure style or black-figure ceramic (Noble 1965). The decor was painted with a liquid fine clay preparation, which becomes black during the firing while the non-painted surface of vessel appears red. The end of the heating step was performed under reducing conditions (smoke) at a temperature high enough to glaze

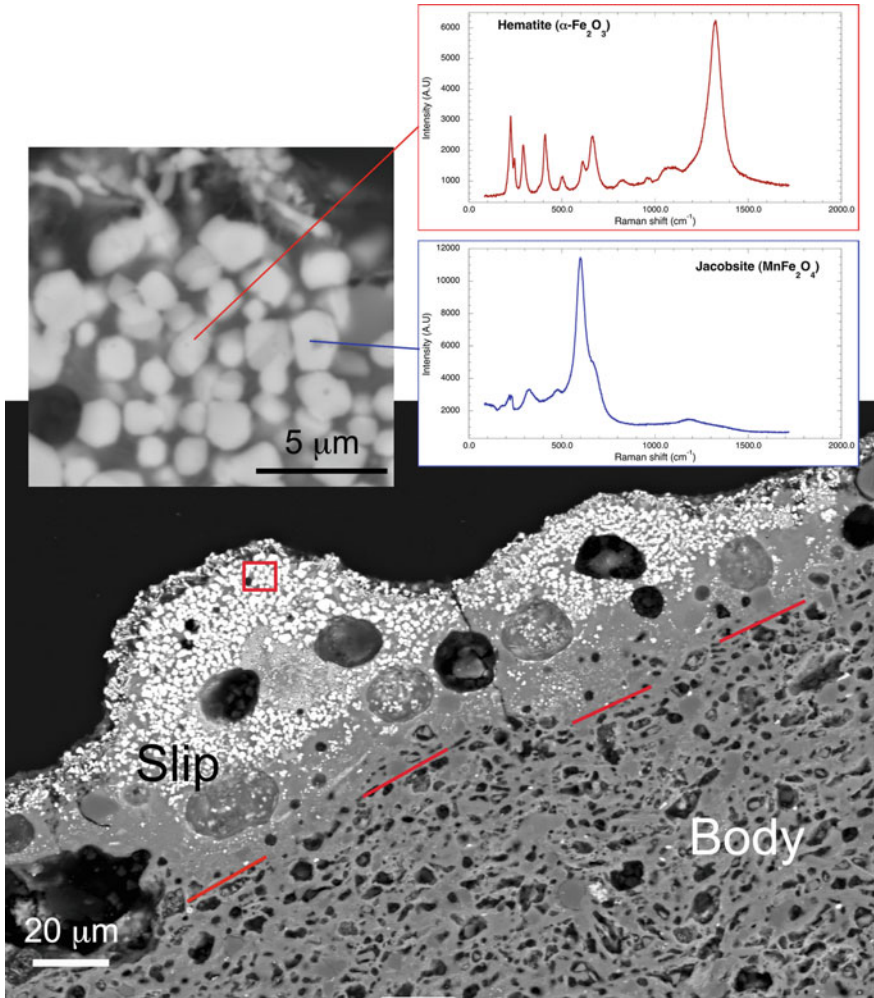


**Fig. 3** Cross-section of a black decor of a Cucuteni ceramic containing both hematite and jacobsite crystals

the painted zones but not enough to glaze the non-painted zones. Then an oxidizing step at lower temperature was performed in order to oxidize the non-glassy zones. Around the last quarter of the 6th century BC, a new style appeared in Athens, which consisted of inverting the colours: the background is black while the figures are red (Fig. 4). To strengthen the red colour of non-glossy zones, fine clay preparations were sometime affixed to these zones. It is specially the case of Attic pottery with coral red slip (Walton et al. 2009). The achievement of such pottery requires a perfect mastery of firing protocol but also the use of two different clay preparations. The clay preparation used for the red zones must have a glassy

**Fig. 4** Attic ceramic of the red figure type (5th c. BC) found in Lattes (France) and described in Chazalon (2010). (Micrograph, courtesy E. Gailledrat)



temperature higher than the one used for the black zones so that only the black zones are glassy during the reducing heating step. These two clay preparations can be obtained, or not, from the same raw clay material. Walton et al. showed that the clay preparations used for red parts had either a higher Ca rate or (and) a larger particle size, so that after the reducing heating step these zones have a higher porosity than the black zones and they can be re-oxidized during the next step.

However, a recent study concerning an attic vase of 5th century attributed to Berlin Painter revealed that this vessel was not obtained using the three phase firing protocol (Cianchetta et al. 2015). It presents a complicated layered architecture of black and red gloss, which seems to require multiple rounds of painting/firing to be achieved. The use of multiple firing was previously suggested on the basis of replication investigations (Walton et al. 2013). Studies are currently underway on the firing protocol of the Attic red-figure ceramics, which could have been more complex than considered until now. Although these potteries were made by civilizations where writing was commonly used, no details were found up to now in antique writings concerning their firings. They are only mentioned on a few drawings on terracotta slabs called “pinakes” and in only one poem (Jubier-Galinier et al. 2003; Lyons 2005; Sciau and Goudeau 2015).

Besides the red-figure ceramics, a lot of tableware was made without decorations and with only a high-gloss black coating. This tradition of black coating vessels was continuous during the Roman Republic period and gave the Campanian tableware, which archaeologists divided into 3 classes (A, B and C) based on the aspect, the period and the production zone. These potteries were produced in Italy (Campania, Etruria) and widely exported in the Mediterranean, in particular in The Gulf of Lion or along Balearic seacoasts. C type is of lower quality with coatings scarcely sintered and thicker (Mirti and Davit 2001). The clay preparations used for their coatings had generally a particle size lightly superior to the one used for Attic production and the firing temperatures were higher (Vendrell-Saz et al. 1991). From a recent study, a firing protocol including a heating step under reducing conditions (mainly at the end of the step) followed by oxidizing cooling allows for obtaining this type of production (Meirer et al. 2013).

**Fig. 5** Terra Sigillata vessel (Drag. 29, 1st c. AD) found in La Graufesenque workshop. (Micrograph, courtesy A. Verhnet)



During the latter half of the first century BC, started in central Italy, tableware with a very high-gloss red coating, also called *Terra Sigillata* or *Samian ware*. Terra Sigillata pottery (Fig. 5) was the most famous tableware produced during the Roman period owing to the mass production of standardized shapes and the widespread distribution of the vessels (Hartley 1971). The beautiful ceramics were characterized by their reddish coloration, glossy coating, and the unique ornamentation created by the use of moulds and stamps (*sigilla*). The success of this pottery led to the rapid spreading of the technique outside the Italic peninsula and from the beginning of the first century AD, large production centres were set up in southern Gaul in such sites as La Graufesenque (Schaad 2007). From the latter half of the 1st century AD, workshops were developed in Spain maybe with the help of Gallic potters (Keay 1988). During the 2nd century AD, the production of southern Gallic workshops drops sharply and a new large workshop was established in central Gaul (Lezoux). Within 3rd and 4th centuries, the Gallic production of Terra Sigillata was moved to eastern Gaul but with a drop in quality. The coatings produced during the 4th century are very little vitrified and their red colours come mainly from a re-oxidation during the last step of firing process. Sigillata or related productions of lesser quality were manufactured in other zones of Roman Empire, mainly from the 2nd century AD.

### 3.2 *Composition and Structure*

As mentioned in the Sect. 3.1, the manufacturing of these high gloss coatings concerns both a wide time period and a large geographic area. Also, it is no question here to describe exhaustively the composition and structure of the different coatings produced but just to give some of their characteristics through a few examples (Table 1). Inside a type, significant differences appear among the various workshops

**Table 1** Examples of the elemental composition ( $\%_{\text{mass}}$ ) of coatings determined by electron microprobe (*Géosciences Environnement Toulouse* (GET) of Toulouse University)

|                   | Na <sub>2</sub> O | MgO            | Al <sub>2</sub> O <sub>3</sub> | SiO <sub>2</sub> | P <sub>2</sub> O <sub>5</sub> | K <sub>2</sub> O | CaO            | TiO <sub>2</sub> | MnO            | Fe <sub>2</sub> O <sub>3</sub> | BaO            | Total |
|-------------------|-------------------|----------------|--------------------------------|------------------|-------------------------------|------------------|----------------|------------------|----------------|--------------------------------|----------------|-------|
| Attic<br>(10)     | 0.51<br>(0.18)    | 2.05<br>(0.17) | 27.83<br>(1.08)                | 45.28<br>(0.93)  | 0.19<br>(0.05)                | 5.75<br>(0.69)   | 0.45<br>(0.19) | 0.65<br>(0.14)   | 0.08<br>(0.03) | 16.35<br>(0.56)                | 0.01<br>(0.01) | 99.2  |
| Camp A<br>(8)     | 2.09<br>(0.36)    | 1.68<br>(0.45) | 28.29<br>(0.63)                | 44.97<br>(0.80)  | 0.16<br>(0.02)                | 4.67<br>(0.40)   | 0.93<br>(0.15) | 0.60<br>(0.11)   | 0.17<br>(0.05) | 15.91<br>(1.00)                | 0.08<br>(0.02) | 99.6  |
| Camp B<br>(11)    | 0.71<br>(0.19)    | 2.26<br>(0.07) | 27.92<br>(0.43)                | 46.47<br>(0.70)  | 0.15<br>(0.02)                | 6.59<br>(1.18)   | 0.79<br>(0.16) | 0.48<br>(0.03)   | 0.10<br>(0.03) | 14.27<br>(1.50)                | 0.07<br>(0.02) | 99.8  |
| TS Italic<br>(39) | 0.94<br>(0.37)    | 3.19<br>(0.45) | 26.64<br>(0.60)                | 48.97<br>(0.77)  | 0.12<br>(0.02)                | 6.51<br>(0.90)   | 1.51<br>(0.90) | 0.57<br>(0.08)   | 0.07<br>(0.02) | 10.27<br>(0.61)                | 0.09<br>(0.02) | 98.9  |
| TS Gaul<br>(72)   | 0.08<br>(0.06)    | 0.94<br>(0.22) | 22.87<br>(2.37)                | 54.86<br>(2.79)  | 0.17<br>(0.04)                | 7.90<br>(0.85)   | 1.37<br>(0.87) | 0.71<br>(0.10)   | 0.05<br>(0.01) | 9.49<br>(1.00)                 | 0.08<br>(0.02) | 98.5  |

The standard deviations are given in brackets as well as the number of samples. The attic and Campanian ceramics were provided by the *laboratoire d'Archéologie des Sociétés Méditerranéennes* and come from the Lattes and Narbonne excavations respectively. The terra sigillata data were extracted from Leon's work (Leon et al. 2015)

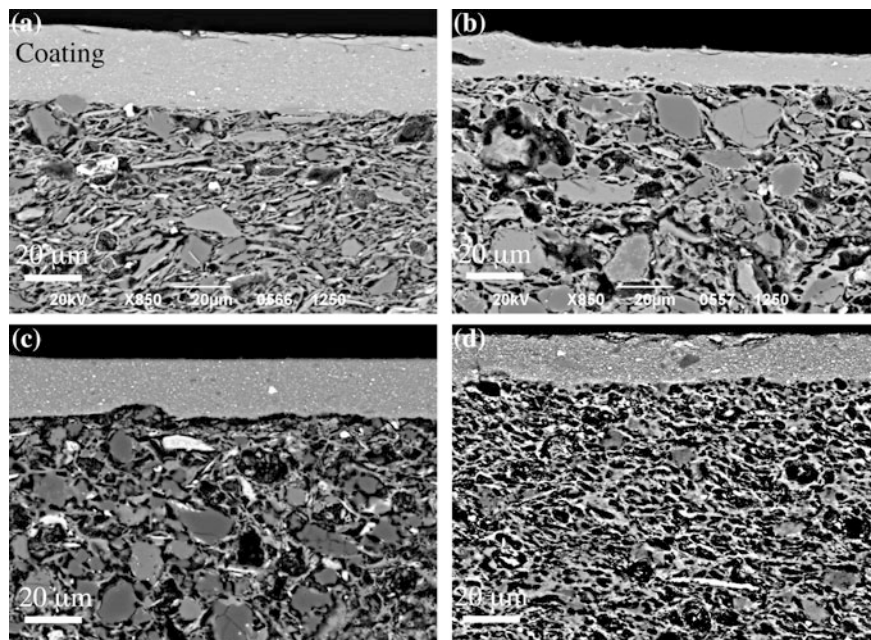


**Fig. 6** Cross-sections of various ceramic types: **a** Attic, **b** Campanian B, **c** Italic Terra Sigillata and **d** Gallic Terra Sigillata

as one can observe comparing the elemental compositions of two main italic workshops (Arezzo, Pisa) of Terra Sigillata and the one (La Graufesenque) of the main southern Gallic workshops. In some cases, the discrimination can be finer and allows for separating the production of an individual pottery-making firm inside the same workshop. For example at Arezzo, the products of “Ateius” can be separated from the one of “Perrenius” on the basis of their element compositions (Leon et al. 2015). Of course, it is also the case for other ceramic types. However even if the Table 1 does not give an exhaustive view of coating compositions, some information can be retrieved (drawn). All these coatings present a low Ca rate (<2 %) and a high rate of Fe and K. The Al/Si ratio is also very similar. Only the coatings of Terra Sigillata made in Gaul contain more silicon oxide. These coatings were obtained from a less fine clay preparation containing a few more quartz crystals. The Fe amount is higher for the black coatings (Attic and Campanian) while the Ca rate is a little higher in the red coatings (Terra Sigillata). The slight deficiency in potassium of Campanian type A was already reported and is a characteristic of these products (Mirti and Davit 2001).

Observed in cross-section using a scanning electron microscope, these diverse ceramics show quite similar structure. The coating appears as a thin layer of a few tens of micrometres denser and much more homogeneous than the body (Fig. 6). The grain size difference between the materials used for the coating and the body is

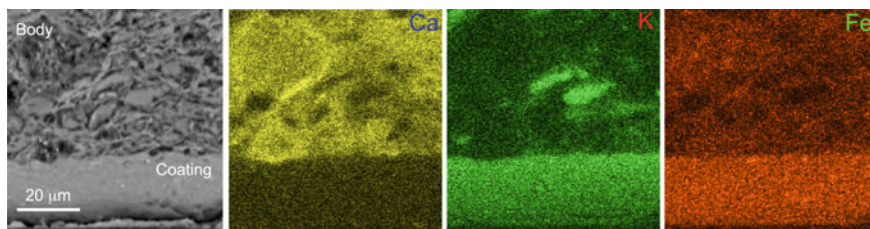


**Fig. 7** Elemental maps recorded on a cross-section of an Attic ceramic. The coating contains more iron and potassium and less calcium than the body

evident. Large crystals of tempers (“non-plastic” phases, such as quartz, feldspars...) are observed in the bodies while only a few small quartz crystals are noticeable in the Gallic Terra Sigillata coatings. The differences in composition between the bodies and coatings are also clearly shown in the elemental maps (Fig. 7) obtained using energy-dispersive X-ray spectroscopy (SEM-EDX). All bodies of these diverse potteries were made from calcareous clay containing tempers of small grain size (a few tens microns).

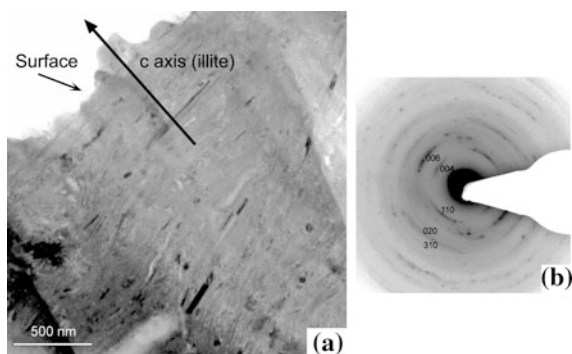
### 3.3 Phase Transformations During Firing

During firing, only the concentration of atoms (H, C, O, Cl, S,...) of volatile elements (water, organic material, carbonate, chlorides, sulphites,...) is changed. The ratio of the other elements (Si, Al, Mg, Ca, Fe,...) is slightly or not modified by the firing process. By contrast, the structural organization (the nature of crystallographic phases) is greatly changed during the firing. The clay minerals (kaolinite, illite, smectite,...) begin to lose water with the elevation of temperature, leading then to structural disruptions. The decomposition produces various new crystalline (mullite, alumina, spinel...) or disordered (glass) phases depending on the nature of clay minerals (McConville and Lee 2005; Lee et al. 2008). Clay minerals can also react with other mineral phases such as hydro-oxides, oxides or carbonates present in the non-fired pottery, to form new phases such as pyroxene, plagioclase, iron oxide,... (Maggetti 1982). The chemical reactions taking place during the firing of a pottery are very diverse and depend, of course, on the chemical and crystallographic composition, but also on the size and spatial distribution of crystallites (heterogeneity) in the starting mixture. Firing atmosphere (reducing or oxidizing) has also a significant influence on the formation of the crystals containing transition metal elements such as the iron oxides. Many of these reactions are irreversible and this great diversity can be considered as an advantage, which can be used to obtain extensive information from the study of pottery fragments.

The firing conditions are seldom suitable for growing large crystals and then only nanometric or submicrometric crystallites are formed. It is particularly true for

**Fig. 8** Example of a non-glassy coating of the Roman period fired at a low temperature (<850 °C).

**a** Bright field TEM image of a cross section showing the microstructure of oriented dehydrated-illite crystals.  
**b** SA electron diffraction pattern of the same area showing the orientation and also the badly crystallisation



the high gloss coatings. The clay preparations used were essentially composed of clay minerals and badly crystallized iron oxides and hydro-oxides. The  $\text{SiO}_2/\text{Al}_2\text{O}_3$  ratios measured in the black coatings [Attic (1.6), Campanian A (1.6) and Campanian B (1.7)] are between those of kaolinite (1.2) and illite (2.2) values. This indicates that the mixtures used for their manufacturing contained mainly these two phases in addition to iron based phases. The ratios are higher in the Terra Sigillata red coating according to higher illite fraction. In contrast to kaolinite, illite contains potassium and the increase of K rate is also in agreement with an increasing account of illite. The high proportion of illite is also confirmed by the observation performed on badly fired ceramics (Fig. 8).

The temperature was not high enough to destroy all illite crystals. This type of image reveals also the organization of illite crystals before firing due to their plate-shape and the use of a liquid preparation in which the thin particles are in suspension and homogeneously distributed. This regular organization allows for obtaining a shiny appearance with only a partial vitrification. The clay crystals are distributed on the surface of the pottery somewhat like tiles on a roof and a beginning of vitrification is enough to make rather dense and not too rough coatings. Of course, the very shiny coating of high quality ceramics requires a further glazing but thanks to this particle organization, it can be obtained at quite low temperatures (850–1000 °C) depending on the composition (K, Na, Mg rates) and the atmosphere (oxidizing or reducing). Above 850 °C, the tetrahedral ( $\text{SiO}_4^{4-}$ ) layers of illitic structure begin to create the glassy matrix while a part of octahedral ( $\text{AlO}_6^{9-}$ ) layers contributes to the formation of various spinel structure types depending on the other elements (Fe, Mg) substituted to Al and/or present in surrounding particles such as iron oxides. For instance, the presence of Mg leads to  $\text{MgAl}_2\text{O}_4$  spinel growth which in turn decreases the Al rate in destroyed illite cluster structure promoting then the glassy matrix (Sciau et al. 2008). Under reducing conditions a second process takes place. The iron oxides/hydroxides are transformed into FeO, which reacts with Al atoms of the illite decomposed structure to form hercynite spinel structure ( $\text{FeAl}_2\text{O}_4$ ). Here again, the hercynite formation facilitates the formation of the glassy matrix. Since the Fe rate is much higher than the Mg rate, the second mechanism is more efficient and can also concern Al atoms

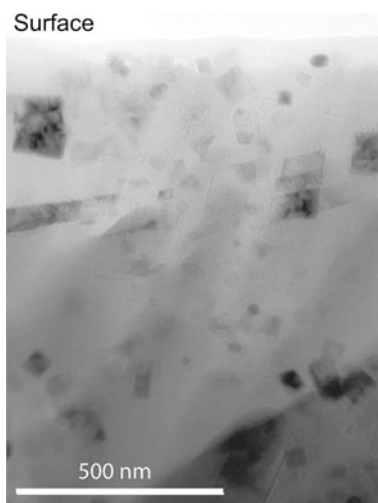
contained in metakaolin clusters. Above 600 °C, kaolinite has lost all constitutional OH groups and the dehydroxylated product is often referred to as metakaolin (Deer et al. 1992; Lee et al. 2008). Under oxidation conditions, iron oxides/hydroxides are transformed into  $\text{Fe}_2\text{O}_3$ , which is a stable form and does not react with Al. Only the formation of  $\text{MgAl}_2\text{O}_4$  spinel can lower the vitrification temperature. In the absence of Mg atoms, the dehydration of K-rich illite leads to the formation of an intermediate potassium aluminium silicate phase (of  $\text{KAl}_3\text{Si}_3\text{O}_{11}$  type) above 800 °C. For temperatures higher than 950 °C, this phase begins to lose its crystallographic long range order and gives between 1000–1100 °C a glassy matrix containing corundum ( $\alpha\text{-Al}_2\text{O}_3$ ) nanocrystals (Sciau et al. 2008).

### 3.4 Nanocrystals and Physical Properties

Observed in transmission electron microscopy, the high gloss coatings are constituted of a glassy matrix containing mainly nano and submicrometric crystals. A few micrometric quartz crystals can also be observed especially in Gallic Terra Sigillata coatings.

The nanometric crystals of black coatings are essentially hercynite (Fig. 9), which gives the colour of these coatings. X-ray diffraction and Raman spectroscopy revealed also the presence of magnetite, but mainly in the coating surface. The presence of maghemite ( $\gamma\text{-Fe}_2\text{O}_3$ ) was also reported in the top layer of some Campanian B coatings and was attributed to a re-oxidation of the surface during the cooling phase. The density of hercynite crystals is sufficient to give a dark black colour and the presence of a few maghemite crystals in surface has no influence on the colour. In fact, the distribution of crystals containing Fe atoms is mostly useful to rebuild the firing process (Meirer et al. 2013).

**Fig. 9** Hercynite crystals observed by TEM in a high gloss coating of a Campanian of type B



The influence of crystal parameters (size, composition, spatial distribution) is more significant for red coatings. In these coatings, the colour is due to hematite but the crystal size, the composition and the homogeneity of repartition in the glassy matrix define the hue. Absorption of hematite in visible spectrum is high and the crystal size plays a major role on the colour hue. Micrometric crystal gives a dark colour while large crystals appear black with a metallic glint. The characteristic red colour of sigillata requires nanometric crystals. However investigations revealed that the hematite crystals grown in sigillata coating contain Al in substitution to Fe (Sciau et al. 2006). This substitution lowers the absorption and allows for obtaining the same colour with submicrometric crystals.

Gallic Terra Sigillata were fired at higher temperatures (around 1050 °C) than the Italic Terra Sigillata (950–1000 °C). This results in a slight increase of the average size of hematite crystals (30 → 50 nm), but this effect is balanced both by the lower crystal density (Fe rate is lower in Gallic Terra Sigillata) and a higher Al substitution (around 8–9 % in Gallic Terra Sigillata). Recent studies showed that the rate of substitution increases with the temperature and that the rate value was higher in Gallic productions than in Italic ones (Leon et al. 2010, 2015). One consequence is that the two types of production present similar colours. In contrast, their mechanical properties are quite different. The higher firing temperature of Gallic products leads to a partial vitrification of their body, which results in a better adherence of coatings. These coatings (Fig. 10) are almost free of spinel in agreement with their low Mg rate, but contain a lot of corundum ( $\alpha$ -Al<sub>2</sub>O<sub>3</sub>) nanocrystals (average size 20 nm). X-ray diffraction and electron energy loss spectroscopy revealed that these crystals contained around 8–9 % Al in substitution to Fe [(Al<sub>0.92</sub>Fe<sub>0.08</sub>)<sub>2</sub>O<sub>3</sub>, Fig. 11]. The presence of iron confers a yellowish colour to this phase, as can be found in the gemmological varieties of this mineral. However, the colour arises mainly from the iron atoms in octahedral coordination in the hematite structure. Actually, the main effect of corundum is to turn the slip into a mechanically strong coating (Sciau et al. 2006).

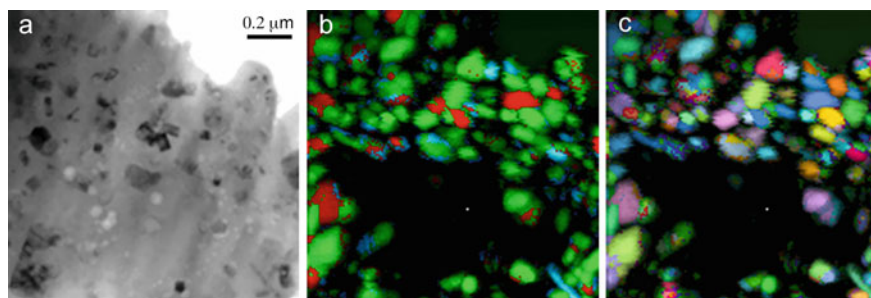


**Fig. 10** Gallic terra sigillata coating observed in TEM. **a** Bright field image, ASTAR high resolution phase **(b)** and orientation **(c)**. The coating **b** consists of hematite (in red), corundum (in green) and spinel (in blue) crystals in a glass matrix. There is no particular orientation of crystals **(c)**

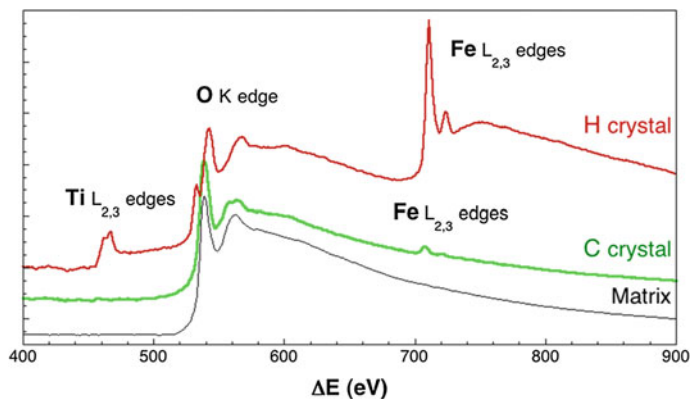


**Fig. 11** EELS analysis of the matrix, hematite and corundum crystals in a Gallic terra sigillata coating

## 4 Iron Oxides in Black Glazed Chinese Ceramics

A rare and metastable ferric oxide polymorph ( $\epsilon$ - $\text{Fe}_2\text{O}_3$ ) has just been discovered in ancient Chinese ceramics (Dejoie et al. 2014). Identified in 1934, this phase keenly interests the materials science community for its promising applications in the fields of electronic storage media and magnetic stripe cards. It exhibits a giant coercive field at room temperature, millimetre-wave ferromagnetic resonance, and magneto-electric coupling (Gich et al. 2006; Tucek et al. 2010). It is the only single metal oxide to accumulate such magnetic/electric properties. Unfortunately, this phase is metastable and its crystal growth is very difficult to obtain. Up to now only nanoscale crystals (nanoparticles, nanowires, thin films) have been obtained (Tronc et al. 1998; Gich et al. 2010).

Black-glazed Jian ware of the Chinese Song dynasty (960–1279 AD) was known for its lustrous black, which could exhibit various coloured patterns. The variety called “hare’s fur” was the most famous and common pattern (Li et al. 2008). Its shining black slip reveals fine radial rust-coloured streaks. Much less prevalent, the variety called “oil spot” was also sought for its silvery glints. Recently, one fragment of each variety was analysed using a set of characterization techniques including micro X-ray fluorescence and micro X-ray diffraction synchrotron, Raman spectroscopy and transmission electron microscopy (Dejoie et al. 2014). It was established that the coloured patterns were due to the crystallization of iron oxides in the glaze surface (Li et al. 2008), but without considering that the predominant form was  $\epsilon$ - $\text{Fe}_2\text{O}_3$ . In the “hare’s fur” variety, the epsilon phase is associated with the alpha form (hematite) while at the surface of the “oil spot” sample, only  $\epsilon$ - $\text{Fe}_2\text{O}_3$  phase was found. The sub-micrometric crystals are concentrated in the oil spots (bubbles arrive at the surface during the firing) and organized in dendritic networks. A majority of these networks are very regular and define quasi perfect 2D gratings (Fig. 12), which behave as dispersive elements leading to

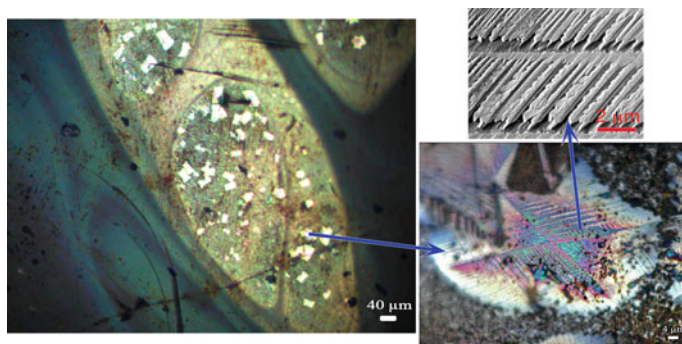


**Fig. 12** Optical and SEM images of the  $\epsilon$ - $\text{Fe}_2\text{O}_3$  crystals observed at the surface of a black-glazed Jian ware of the “oil spot” type (Song dynasty: 960–1279 AD)

the creation of structural colours through interference effects (Zuppiroli et al. 2003). These colours, which depend on angular lighting conditions, are very brilliant and iridescent with blue to red variations as shown in Fig. 12.

This organization of sub-micrometric crystals can be related to 2D photonic crystals (Joannopoulos et al. 1997) where a periodic array of nanoparticles affect the motion of photons (visible light) in the same way that a tri-periodic atom arrangement (standard crystal) affects X-rays. In fact, these dendritic networks are rather similar to the structure which can be found in nature in feathers of birds or scales of butterflies showing iridescent colours (Kinoshita and Yoshioka 2005).

## 5 Conclusion

In this chapter, we have shown that the nanoscale crystals present in the coatings of Greek and Roman potteries are responsible for their colour features and also contribute to their mechanical properties. For instance, the high hardness of Gallic sigillata coatings is due to nanocrystals of corundum homogeneously dispersed in the glassy matrix. Actually, nanocrystals and/or sub micrometric crystals play a significant role in the colour feature of several decorative layers of ancient potteries such as the copper crystals in the oxblood glaze or blue cobalt particles ( $\text{CoAl}_2\text{O}_4$  spinel phase) in blue and white porcelains and other blue colours underglaze (Wang and Wang 2011; Figueiredo et al. 2012).

The study of nanocrystals present in ceramic coatings is also a powerful way to obtain relevant information concerning the manufacturing processes. Thus the different steps of the firing of some Greek and Roman ceramics were clarified from the study of Fe-based particles. It was shown that the Al/Fe substitution in hematite structure influences the tin colour and depends on the firing temperature. An ongoing study seems to indicate that the blue cobalt particles are also substituted in

blue decorations of Qinghua porcelains (Wang et al. 2016). Indeed, the majority of crystallographic phases formed during the firing of potteries are substituted. The nature and rate of the substitution depend both on the raw material composition and the firing conditions. An in depth study of these parameters could provide new significant information concerning manufacturing process. The current analytical facilities allow us to perform such studies on nanocrystals. Hopefully, these relevant data should be available in a near future.

**Acknowledgments** The author gratefully acknowledge Eric Gailledrat, Cécile Jubier-Galinier and Corinne Sanchez (laboratoire Archéologie des Sociétés Méditerranéennes, UMR 5140) and Dragomir Nicolae Popovici (National Museum of Romania's History) for the archaeological samples as well as Philippe de Parseval (GET, Toulouse University) for the elemental composition measurements, Christophe Deshayes (CEMES) for SEM investigations and Sébastien Joulie (CEMES) for TEM-ASTAR investigations. I would also like to thank Deborah Decamaret and Philippe Goudeau for their help. This article was partially funded by the ARCHIMEDE Labex programme: Investissement d'Avenir ANR-11-LABX-0032-01.

## References

- Angelini I, Artioli G, Bellintani P, Diella V, Gemmi M, Polla A, Rossi A (2004) Chemical analyses of bronze age glasses from Frattesina di Rovigo, northern Italy. *J Archaeol Sci* 31(8):1175–1184. doi:[10.1016/j.jas.2004.02.015](https://doi.org/10.1016/j.jas.2004.02.015)
- Barber DJ, Freestone IC (1990) An investigation of the origin of the color of Lycurgus cup by analytical transmission electron-microscopy. *Archaeometry* 32:33–45
- Brun N, Mazerolles L, Pernot M (1991) Microstructure of opaque red glass containing copper. *J Mater Sci Lett* 10(23):1418–1420. doi:[10.1007/BF00735696](https://doi.org/10.1007/BF00735696)
- Bugoi R, Constantinescu B, Pantos E, Popovici D (2008) Investigation of Neolithic ceramic pigments using synchrotron radiation X-ray diffraction. *Powder Diffr* 23(3):195–199
- Chazalon L (2010) Les céramiques attiques du Ve s. av n.è à Lattes. Première données sur le cinquième siècle avant notre ère dans la ville de Lattara, ADAL, Lattes (Lattara 21) 2:1.5, 618
- Cianchetta I, Trentelman K, Maish J, Saunders D, Foran B, Walton M, Sciau P, Wang T, Pouyet E, Cotte M, Meirer F, Liu Y, Pianetta P (2015) Evidence for an unorthodox firing sequence employed by the Berlin painter: deciphering ancient ceramic firing conditions through high-resolution material characterization and replication. *J Anal At Spectrom* 30:666–676. doi:[10.1039/C4JA00376D](https://doi.org/10.1039/C4JA00376D)
- Colomban P (2009) The use of metal nanoparticles to produce yellow, red and iridescent colour, from bronze age to present times in lustre pottery and glass: solid state chemistry, spectroscopy and nanostructure. *J Nano Res* 8:109–132
- Colomban P, Liem NQ, Sagon G, Tinh HX, Hoanh TB (2003) Microstructure, composition and processing of 15th century Vietnamese porcelains and celadons. *J Cult Herit* 4(3):187–197. doi:[10.1016/s1296-2074\(03\)00045-1](https://doi.org/10.1016/s1296-2074(03)00045-1)
- Deer WA, Howie RA, Zussman J (1992) An introduction to the rock-forming minerals. Pearson, Harlow
- Dejoie C, Sciau P, Li WD, Noe L, Mehta A, Chen K, Luo HJ, Kunz M, Tamura N, Liu Z (2014) Learning from the past: rare epsilon-Fe<sub>2</sub>O<sub>3</sub> in the ancient black-glazed Jian (Tenmoku) wares. *Sci Rep* 4:4941. doi:[10.1038/srep04941](https://doi.org/10.1038/srep04941)
- Figueiredo MO, Silva TP, Veiga JP (2012) A XANES study of cobalt speciation state in blue-and-white glazes from 16th to 17th century Chinese porcelains. *J Electron Spectrosc Relat Phenom* 185(3–4):97–102. doi:[10.1016/j.elspec.2012.02.007](https://doi.org/10.1016/j.elspec.2012.02.007)

- Freestone I, Meeks N, Sax M, Higgitt C (2007) The Lycurgus cup—a Roman nanotechnology. *Gold Bull.* 40(4):270–277
- Garcia D, d' Anna A, Desbat A, Schmitt A, Verhaeghe F (2014) *La Céramique: La poterie du Néolithique aux temps modernes*. Editions Errance
- Gich M, Frontera C, Roig A, Fontcuberta J, Molins E, Bellido N, Simon C, Fleta C (2006) Magnetolectric coupling in epsilon-Fe<sub>2</sub>O<sub>3</sub> nanoparticles. *Nanotechnology* 17(3):687–691. doi:[10.1088/0957-4484/17/3/012](https://doi.org/10.1088/0957-4484/17/3/012)
- Gich M, Gazquez J, Roig A, Crespi A, Fontcuberta J, Idrobo JC, Pennycook SJ, Varela M, Skumryev V (2010) Epitaxial stabilization of epsilon-Fe<sub>2</sub>O<sub>3</sub> (001) thin films on SrTiO<sub>3</sub> (111). *Appl Phys Lett* 96(11):112508. doi:[10.1063/1.3360217](https://doi.org/10.1063/1.3360217)
- Hartley BR (1971) *Roman Samian Ware: Terra Sigillata*. Herts Archaeol Soc
- Joannopoulos JD, Villeneuve PR, Fan SH (1997) Photonic crystals: putting a new twist on light. *Nature* 386(6621):143–149. doi:[10.1038/386143a0](https://doi.org/10.1038/386143a0)
- Jubier-Galinier C, Laurens A-F, Tsingarida A (2003) Les atelier de potiers en attique. In: Rouillard P, Verbanck-Pierard A (eds) *Le vase grec et ses destins*. Biering and Brinkmann, Munich, pp 27–43
- Keay SJ (1988) *Roman Spain*. University of California Press, California
- Kinoshita S, Yoshioka S (2005) Structural colors in nature: the role of regularity and irregularity in the structure. *Chem Phys Chem* 6(8):1442–1459. doi:[10.1002/cphc.200500007](https://doi.org/10.1002/cphc.200500007)
- Lee WE, Souza GP, McConville CJ, Tarvornpanich T, Iqbal Y (2008) Mullite formation in clays and clays-derived vitreous ceramics. *J Eur Ceram Soc* 28:465–471
- Leon Y, Lofrumento C, Zoppi A, Carles R, Castellucci EM, Sciau P (2010) Micro-Raman investigations of terra sigillata slips: a comparative study of central italian and southern Gaul productions. *J Raman Spectrosc* 41(11):1550–1555
- Leon Y, Sciau P, Passelac M, Sanchez C, Sablayrolles R, Goudeau P (2015) Evolution of terra sigillata technology from Italy to Gaul through a multi-technique approach. *J Anal At Spectrom* 30(3):658–665. doi:[10.1039/C4JA00367E](https://doi.org/10.1039/C4JA00367E)
- Li WD, Luo HJ, Li JN, Li JZ, Guo JK (2008) Studies on the microstructure of the black-glazed bowl sherds excavated from the Jian kiln site of ancient China. *Ceram Int* 34(6):1473–1480. doi:[10.1016/j.ceramint.2007.04.004](https://doi.org/10.1016/j.ceramint.2007.04.004)
- Lions CL (2005) The Greek vase and its destinies. *Am J Archaeol* 109(1):113–114
- Maggetti M (1982) Phase analysis and its significance for technology and origin. In: Olin JS, Franklin AD (eds) *Archaeological ceramics*. Smithsonian Institution Press, Washington DC, pp 121–133
- McConville CJ, Lee WE (2005) Microstructural development on firing illite and smectite clays, compared with that in kaolinite. *J Am Ceram Soc* 88(8):2267–2276
- Meirer F, Liu YJ, Pouyet E, Fayard B, Cotte M, Sanchez C, Andrews JC, Mehta A, Sciau P (2013) Full-field XANES analysis of Roman ceramics to estimate firing conditions—a novel probe to study hierarchical heterogeneous materials. *J Anal At Spectrom* 28(12):1870–1883
- Mirti P, Davit P (2001) Technological characterization of Campanian pottery of type A, B and C and of regional products from ancient Calabria (southern Italy). *Archaeometry* 43:19–33. doi:[10.1111/1475-4754.00002](https://doi.org/10.1111/1475-4754.00002)
- Nakai I, Numako C, Hosono H, Yamasaki K (1999) Origin of the red color of satsuma copper-ruby glass as determined by EXAFS and optical absorption spectroscopy. *J Am Ceram Soc* 82(3):689–695
- Noble JV (1965) *The techniques of painted Attic pottery*. Watson-Guption edn, New York
- Picon M, Vernhet A (2008) Les très grands fours à sigillées en Gaule, et notamment à la Graufesenque. SFECAG, actes du Congrès de L'Escala-Empuries, pp 553–566
- Ricciardi P, Colombari P, Tournie A, Macchiarola M, Ayed N (2009) A non-invasive study of Roman Age mosaic glass tesserae by means of Raman spectroscopy. *J Archaeol Sci* 36(11):2551–2559. doi:[10.1016/j.jas.2009.07.008](https://doi.org/10.1016/j.jas.2009.07.008)
- Schaad D (2007) *La Graufesenque (Millau, Aveyron), volume I; Condatomagos une agglomération de confluent en territoire rutène., vol I. La Graufesenque (Millau, Aveyron)*, Editions de la Fédération Aquitania

- Sciau P (2012) Nanoparticles in ancient materials: the metallic lustre decoration of medieval ceramics. In: Hashim AA (ed) *The delivery of nanoparticles*. InTech, pp 525–540. doi:[10.5772/34080](https://doi.org/10.5772/34080)
- Sciau P, Goudeau P (2015) Ceramics in art and archaeology: a review of the materials science aspects. *Eur Phys J B* 88(5):1–11. doi:[10.1140/epjb/e2015-60253-8](https://doi.org/10.1140/epjb/e2015-60253-8)
- Sciau P, Relaix S, Roucau C, Kihn Y (2006) Microstructural and microchemical characterization of roman period terra sigillata slips from archeological sites in southern France. *J Am Ceram Soc* 89(3):1053–1058
- Sciau P, Relaix S, Mirguet C, Goudeau P, Bell AMT, Jones RL, Pantos E (2008) Synchrotron X-ray diffraction study of phase transformations in illitic clays to extract information on sigillata manufacturing processes. *Appl Phys A* 90:61–66
- Tite MS (2008) Ceramic production, provenance and use, a review. *Archaeometry* 50(2):216–231
- Tite MS, Bimson M, Freestone IC (1982) An examination of the high gloss surface finishes on Greek Attic and Roman Samian wares. *Archaeometry* 24:117–126
- Tronc E, Chaneac C, Jolivet JP (1998) Structural and magnetic characterization of epsilon-Fe<sub>2</sub>O<sub>3</sub>. *J Solid State Chem* 139(1):93–104. doi:[10.1006/jssc.1998.7817](https://doi.org/10.1006/jssc.1998.7817)
- Tucek J, Zboril R, Namai A, Ohkoshi S (2010) Epsilon-Fe<sub>2</sub>O<sub>3</sub>: an advanced nanomaterial exhibiting giant coercive field, millimeter-wave ferromagnetic resonance, and magnetoelectric coupling. *Chem Mater* 22(24):6483–6505. doi:[10.1021/cm101967h](https://doi.org/10.1021/cm101967h)
- Vendrell-Saz M, Pradell T, Molera J, Aliaga S (1991) Proto-campanian and A-campanian ceramics: characterization of the differences between the black coatings. *Archaeometry* 33(1):109–117
- Walton MS, Doehne E, Trentelman K, Chiari G, Maish J, Buxbaum A (2009) Characterization of coral red slips on Greek Attic pottery. *Archaeometry* 51(3):383–396
- Walton M, Trentelman K, Cummings M, Poretti G, Maish J, Saunders D, Foran B, Brodie M, Mehta A (2013) Material evidence for multiple firings of ancient athenian red-figure pottery. *J Am Ceram Soc* 96(7):2031–2035
- Wang L, Wang C (2011) Co speciation in blue decorations of blue-and-white porcelains from Jingdezhen kiln by using XAFS spectroscopy. *J Anal At Spectrom* 26(9):1796–1801. doi:[10.1039/c0ja00240b](https://doi.org/10.1039/c0ja00240b)
- Wang T, Sciau P, Feng ZY, Fayard B, Pouyet E, Cotte M, De Nolf W, Zhu TQ (2016) Synchrotron-based multi-analytical study of Chinese Qinghua porcelains (Ming dynasty): micro-composition and chromogenic mechanisms of blue decors. *Anal Chem* (to be published)
- Wood N (1999) *Chinese glazes, their origins, chemistry and recreation*. University of Pennsylvania Press, Philadelphia
- Zuppiroli L, Bussac M-N, Grimm C (2003) *Traité des couleurs*. Presses polytechniques et universitaires romandes, Lausanne



<http://www.springer.com/978-94-6239-197-0>

Nanoscience and Cultural Heritage

Dillmann, P.; Bellot-Gurlet, L.; Nenner, I. (Eds.)

2016, XVI, 311 p. 128 illus., 85 illus. in color., Hardcover

ISBN: 978-94-6239-197-0

A product of Atlantis Press